Comments on Unfolding Methods in ALICE

Jan Fiete Grosse-Oetringhaus for the ALICE collaboration
CERN, Geneva, Switzerland

Abstract
This paper discusses the unfolding methods presently used within ALICE and gives examples of practical issues with unfolding from an experimentalist's point of view.

1 Unfolding Methods

The main unfolding methods used within ALICE are χ^2 minimization with regularization [1] and iterative unfolding based on Bayes' theorem [2, 3]. Both use a detector response matrix which is determined with a Monte Carlo simulation.

In χ^2 minimization with regularization, the binned unfolded spectrum U is found by minimizing

$$\hat{\chi}^2(U) = \sum_m \left(\frac{M_m - \sum_t R_{mt} U_t}{e_m} \right)^2 + \beta F(U), \tag{1}$$

where R is the response matrix, M is the measured spectrum, e is the estimated measurement error, and $\beta F(U)$ is a regularization term that suppresses high-frequency components in the solution. The regularization term imposes assumptions on the shape of the corrected spectrum which are kept to a minimum by just requiring that the corrected spectrum is smooth. The smoothness is imposed by the choice

$$F(U) = \sum_t \frac{(U'_t)^2}{U_t} = \sum_t \frac{(U_{t-1} - U_t)^2}{U_t}, \tag{2}$$

which minimizes the fluctuations with respect to a constant constraint imposed by first derivatives or by

$$F(U) = \sum_t \frac{(U''_t)^2}{U_t} = \sum_t \frac{(U_{t-1} - 2U_t + U_{t+1})^2}{U_t}, \tag{3}$$

which minimizes the fluctuations with respect to a linear constraint imposed by second derivatives.[1] The regularization coefficient β is chosen such that, after minimization, the contribution of the first term in Eq. 1 is of the same order as the number of degrees of freedom (the number of bins in the unfolding).

The second unfolding method is an iterative procedure based on Bayes' theorem using the relations:

$$\tilde{R}_{tm} = \frac{R_{mt} \cdot P_t}{\sum_{t'} R_{mt'} P_{t'}}, \qquad U_t = \sum_m \tilde{R}_{tm} M_m, \tag{4}$$

with an *a priori* distribution P. The result U of an iteration is used as a new *a priori* P distribution for the following iteration. Optionally a smoothing is applied, averaging over adjacent bins:

$$\hat{U}_t = (1 - \alpha) \cdot U_t + \alpha \cdot \frac{1}{3}(U_{t-1} + U_t + U_{t+1}) \tag{5}$$

with $0 \leq \alpha \leq 1$ deciding the level of smoothing. The smoothing as well as limiting the number of iterations regularizes the distribution and reduces the influence of high-frequency oscillation in the solution [4].

[1] The contribution of Eq. (2) and Eq. (3) to Eq. (1) vanishes for a constant and linear solution, respectively.

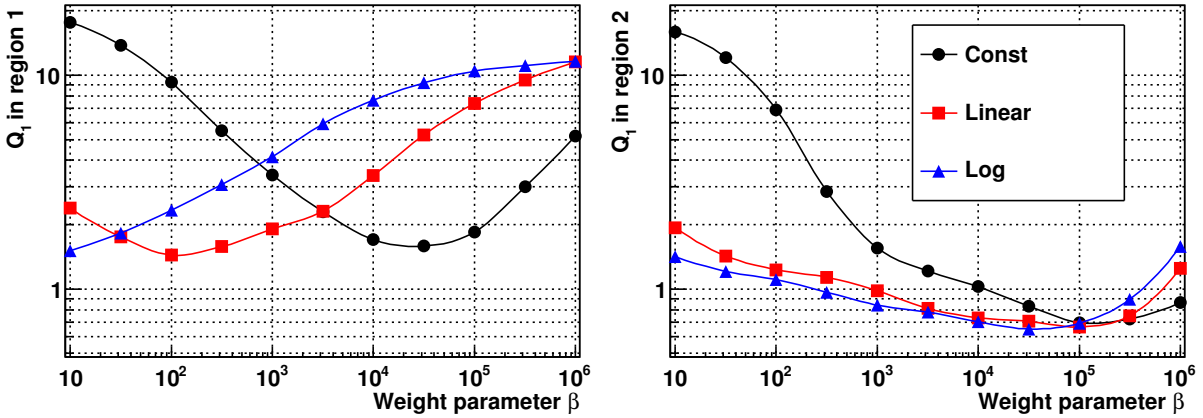

Fig. 1: Performance of the χ^2-minimization. The figure shows the difference between an input distribution and the unfolded distribution ($Q_1 = \langle \frac{|T_t - U_t|}{e_t} \rangle_t$) for a region where the slope changes quickly (left panel) and where the slope is rather constant (right panel) for three different regularizations (Const: Eq. (2), linear: Eq. (3), and log (equation not shown here, see [6]), as function of regularization weight β. The lines are drawn only to guide the eye. Figure from [6].

The bias of the regularization on the unfolded result is evaluated with the prescription given in [5]:

$$b_t = \sum_m \frac{\partial T_t}{\partial M_m} \left(\sum_t R_{mt} U_t - M_m \right) \tag{6}$$

where the derivative is evaluated numerically by unfolding several times while changing M.

1.1 Optimal parameters

While evaluating the regularization term $F(U)$ and the magnitude of β in χ^2 minimization as well as the number of iterations and the smoothing parameter in iterative unfolding, it is important to consider the expected shape of the distribution to be measured. If the distribution has different qualitative behavior in different regions, it is important to study them separately. For the example of the multiplicity distribution, there is a region where the slope changes quickly (at low multiplicity) and a region where the slope is rather constant (at intermediate multiplicities); a third qualitatively different region is at high multiplicities where the statistics is low. Figure 1 shows a MC study where different regularizations are evaluated as a function of β. It can be seen that the optimal parameter β is different for the different regions but only one parameter value can be used in the unfolding for the final distribution. Further, the optimal β for the two shown regions is closer in case of the regularization Eq. (2) than for Eq. (3). Such a conclusion, however, has to be studied using the expected shape of the unfolded distribution. In practice, a range of β values have to be used and the sensitivity to the specific choice has to be addressed in the systematic uncertainties. More details about this evaluation can be found in [6].

2 Applications

Unfolding methods are used among other analyses for the measurement of multiplicity distributions, p_T distributions and the jet spectra. For illustration, the response matrices for the unfolding of the multiplicity distribution and the jet p_T spectrum are shown in Figure 2.

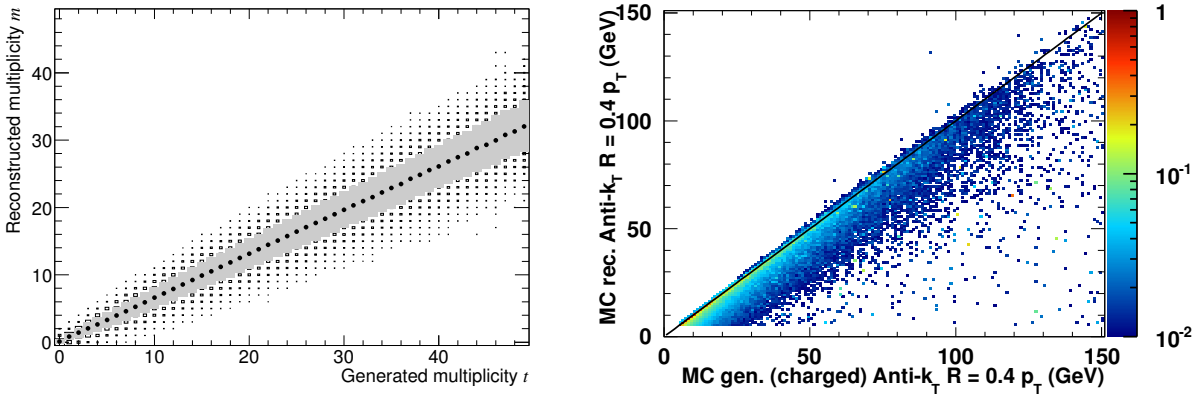

Fig. 2: Graphical representation of detector response matrices. Left panel: number of found tracks (m) vs the number of generated primary particles in $|\eta| < 1.0$ (t). The distribution of the measured tracks multiplicity for a given generated multiplicity shown with its most probable value (dots), r.m.s. (shaded areas), and full spread (squares). Figure from [7]. Right panel: reconstructed vs generated jet p_T found with the anti-k_T algorithm [8] (cone size $R = 0.4$).

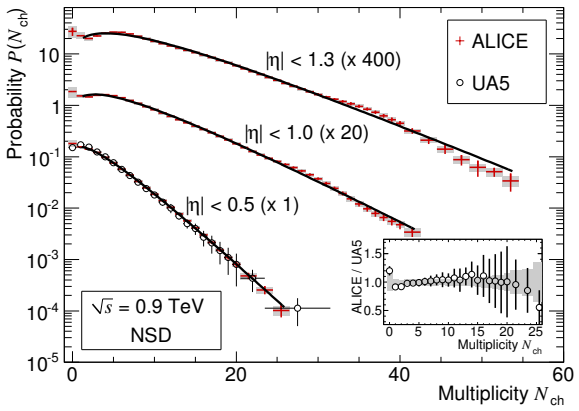

Fig. 3: Multiplicity distributions in three pseudorapidity (η) ranges for non single diffractive events at $\sqrt{s} = 900\,\mathrm{GeV}$. The solid lines show fits with negative binominal distribution. Figure from [7].

3 Residual structures in unfolded results

As discussed earlier regularization reduces the influence of high-frequency fluctuations. Obviously, such structures are not removed completely and depending on the analyzed sample they may still appear quite significant. Figure 3 shows the multiplicity distribution measured by ALICE at $\sqrt{s} = 900\,\mathrm{GeV}$ in different η-regions [7]. The distributions are fitted with negative-binomial distributions which emphasizes small wavy fluctuations in the two larger pseudorapidity intervals at multiplicities above 25. Visually these may appear to be significant, but one needs to note that the errors in the deconvoluted distribution are correlated over a range comparable to the multiplicity resolution (see the left panel of Figure 2).

It is interesting to study if one can attribute such a structure in the unfolded distribution to a structure in the measured distribution. This is done by assuming an exponential shape of the corrected distribution in the corresponding multiplicity range and studying the effect on the residuals. Figure 4 shows in the left panel the residuals of the distribution of Figure 3 in $|\eta| < 1$. The right panel shows the same residuals when an exponential shape of the unfolded distribution in the region around 30 is enforced. One sees that removing the structure from the unfolded result leads to the appearance of a

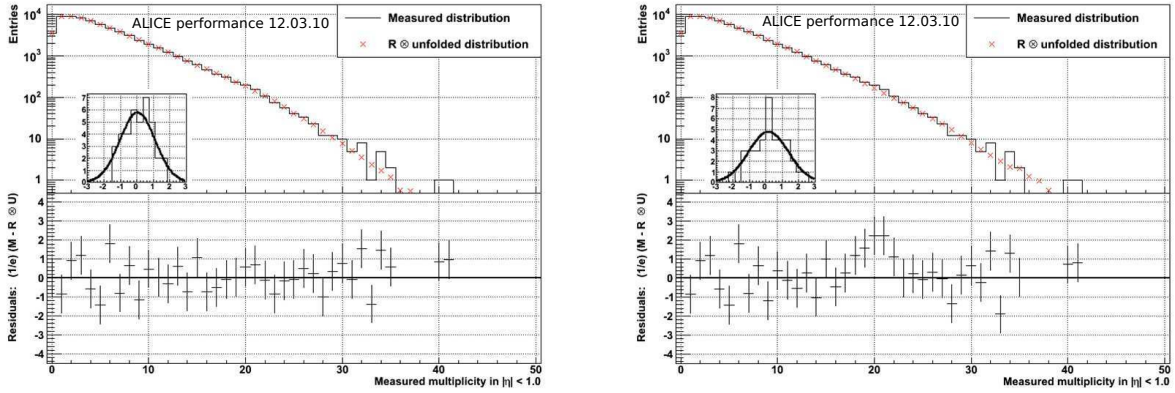

Fig. 4: Measured raw multiplicity distribution (elements of vector M, histogram), superimposed on the convolution $R \otimes U$ of the unfolded distribution with the response matrix (crosses), for $|\eta| < 1.0$ (upper plot). The error bars are omitted for visibility. Normalized residuals, i.e. the difference between the measured raw distribution and the corrected distribution folded with the response matrix divided by the measurement error (lower plot). The inset shows the distribution of these normalized residuals fitted with a Gaussian. The left panel shows the *normal* result while in the right panel an exponential shape is enforced. The small wavy fluctuation in the unfolded distribution (Fig. 3) reappears in the residuals when the exponential is enforced (right panel). For more details see text.

structure in the residuals. However, it is found only in a very few multiplicity bins, clearly less than in the unfolded distributions. This is expected because the response matrix is quite wide (see Figure 2, left panel) and therefore a measured bin can contribute to many unfolded bins. In summary one can learn from this example that a small fluctuation in the measured data can lead to a visually quite appealing structure in the unfolded result. Similar observations for a different deconvolution method were made by UA5 in [9].

References

[1] V. Blobel, in *8th CERN School of Comp. – CSC'84*, Aiguablava, Spain, 9–22 Sep. 1984, CERN-85-09, 88, (1985)

[2] G. D'Agostini, Nucl. Instrum. Meth. A **362**, 487 (1995)

[3] G. D'Agostini, CERN Report CERN-99-03 (1999)

[4] V. Blobel, arXiv:hep-ex/0208022 (2002).

[5] G. Cowan, in *Advanced Statistical Techniques in Particle Physics*, Durham, England, 18-22 Mar 2002, Durham Univ., 248 (2002)

[6] J.F. Grosse-Oetringhaus, PhD thesis, University of Münster, Germany, CERN-THESIS-2009-033 (2009)

[7] ALICE Collaboration, K. Aamodt et al., Eur. Phys. J. C **68** (2010) 89

[8] M. Cacciari and G. P. Salam, Phys. Lett. B **641** (2006) 57

[9] UA5 Collaboration, R.E. Ansorge et al., Z. Phys. C **43**, 357 (1989)